Emerging Materials Research
Volume 1 Issue EMR1
Simulation of device parameters of high efficiency multicrystalline silicon solar cells
Budhraja, Misra and Ravindra
ice | science

Pages 25–32 http://dx.doi.org/10.1680/emr.11.00007
Research Article
Received 06/09/2011 Accepted 08/11/2011
Published online 10/11/2011
Keywords: solar cells/device simulation/silicon

ice Institution of Civil Engineers publishing

Simulation of device parameters of high efficiency multicrystalline silicon solar cells

1 **Vinay Budhraja** PhD
Research Assistant, National Renewable Energy Laboratory, Golden, USA; New Jersey Institute of Technology, Newark, USA

2 **Durgamadhab Misra** PhD
Professor, Electrical and Computer Engineering Department, New Jersey Institute of Technology, Newark, USA

3 **Nuggehalli M. Ravindra** PhD
Professor and Chair, Department of Physics, New Jersey Institute of Technology, Newark, USA

The results of the simulation of the reported experimental results of high efficiency multicrystalline silicon (mc-Si) solar cells, using PC1D software, are reported in this study. Results obtained by various groups have been incorporated and compared in this study. The highest efficiency reported so far for mc-Si solar cells is 20·4% and 17–18% by research laboratories and commercial houses, respectively. The efficiency can be further enhanced if passivation characteristics on both the front and back surface are improved. The role of back surface recombination has become more significant in light of the use of thin mc-Si wafers by the solar cell industry. Based on the passivation characteristics and considering the understanding of the past three decades of studies, the authors have proposed and simulated a structure for mc-Si solar cells to improve the performance of the same. The results of our modeled structure of mc-Si solar cell show an efficiency of 21·88% with *short-circuit current density,* J_{sc} = 39·39 mA/cm², and open circuit voltage, V_{oc} = 0·666 V.

1. Introduction

Multicrystalline silicon (mc-Si) solar cells account for around 50% of the total solar cell production. According to the January 2011 issue of *Solar Industry* (Magazine Article, 2011), mc-Si technology represents roughly 80% of the c-Si market on a dollar per watt basis against three challengers: thin film silicon, CdTe and Copper indium gallium (di) selenide (CIGS). The mc-Si technology will continue to be profitable throughout the value chain from $1·45/W in 2009 to $0·93/W in 2015, assuming polycrystalline silicon (pc-Si) pricing at $70/kg. The cost of mc-Si solar cells is less than monocrystalline silicon solar cells because it is produced from lower grade feedstock and out of spec material from the microelectronics industry. The mc-Si solar cells are the better alternative to monocrystalline silicon because of the tradeoff between cost and efficiency (Tobias *et al.,* 2004). The reasons for the low performance of mc-Si solar cells in comparison to monocrystalline silicon solar cells are: (i) less capability for uniform texturing in mc-Si, (ii) surface passivation of front and back surfaces is still not greatly improved, (iii) defects such as dislocations, grain boundaries, defect clusters etc. are present in mc-Si and (iv) the mechanical strength of mc-Si wafer is less than that of monocrystalline silicon wafer. The advancements in mc-Si solar cell technology for the past three decades, in chronological order, have been reviewed and the advancements in the understanding of defects and characterization techniques have also been discussed (Budhraja *et al.,* 2011a).

In the past three decades, the useful advancements in mc-Si solar cell technology were aimed at improving the efficiency from 6·14% in 1980 to 20·4% in 2004. Here, the authors focus mainly on the modeling of world record cells. Besides the research groups that achieved world record efficiencies in mc-Si solar cells, there were some other groups that reported several new techniques in the processing steps of their mc-Si solar cells. These research groups could not achieve the highest efficiency but their contributions were well accepted in the advancements of mc-Si solar cell technology.

1.1 Brief review of experimental work previously reported by other groups

The cells listed below are those which have been fabricated by various research groups. Most of the processing steps are similar except for several variations used by these groups in process conditions at some steps. The only difference between the multicrystalline silicon (mc-Si) and polycrystalline silicon (pc-Si) is the grain size. The grain size of mc-Si is between 1 mm and 10 cm and the size of grains in pc-Si is between 1 μm and 1 mm, respectively (Basore, 1994).

Cell 1: In 1980, T. Saitoh (Saitoh *et al.,* 1980) achieved 6·14% efficiency in pc-Si solar cells by annealing in N_2 and the efficiency was further increased by increasing the annealing time. It was found that impurity gettering which begins at the wafer surface caused a decrease in junction leakage and enhanced open circuit voltage and fill factor.

Cell 2: In 1984, S. M. Johnson (Johnson *et al.,* 1984) achieved 15·7% efficiency in their pc-Si solar cells. The grain size of the pc-Si wafer was around 0·5 cm. To obtain high efficiency in solar cells, the polycrystalline material was casted in such a way that the base resistivity and other properties, similar to Czochralski silicon, were achieved. Because of this processing step, they called their material semi-crystalline. In this case, two layers (MgF_2 and Ta_2O_5) of AR coating were used. These layers provided an additional advantage for reducing reflectance.

Cell 3: In 1985, S. R. Wenham (Wenham *et al.,* 1985) used plasma treatment in the processing of pc-Si solar cells. They also attempted the same processing steps on their float zone silicon wafers. Plasma processes were performed in three successive steps. Plasma hydrogenation, plasma etching and plasma deposition of AR coating provided advantages such as the increase in short-circuit current density (J_{sc}), contact resistance reduction and an overall improvement in cell parameters, respectively. This process was called passivated emitter solar cell (PESC) because of the passivation of the *n*-region by SiO_2.

Cell 4: One year later, in 1986, S. Narayanan (Narayanan *et al.,* 1986) used phosphorous pretreatment in PESC. Phosphorous pretreatment steps resulted in the improvement in diffusion length and cell parameters.

Cell 5: M.A. Green (Green *et al.,* 1984) were able to increase the efficiency by 1%. They developed buried contact technology in their cell and used laser technique for texturing. The structural rounding in their cell reduced stress concentration and dislocation generation during subsequent oxidation.

Cell 6: In 1993, P. Sana (Sana *et al.,* 1993) reported a 1% increase in efficiency in their cells in which the oxide passivation was performed after phosphorous gettering. Oxide passivation results in an increase in J_{sc} and a decrease in saturation current (I_{01}).

Cell 7: In 1996, A. Rohatgi (Rohatgi *et al.,* 1996) reported 18·6% efficiency in their cells in which the mc-Si was grown by heat exchanger method (HEM). But their process steps were the same as used in OTC (Osaka Titanium Corporation) for mc-Si material. In both OTC and HEM material, the effect of grain boundaries can be neglected because of the large grain size.

Cell 8: In 1998, J. Zhao (Zhao *et al.,* 1998) reported 19·8% efficiency in cells fabricated on honeycomb textured mc-Si. The cell efficiency was improved due to enshrouding cell surfaces in thermally grown oxide and isotropic etching to form a hexagonally symmetric honeycomb surface texture. This group achieved 18·2% efficiency in HEM material using a honeycomb surface texture. This value was still less than the efficiency obtained by Rohatgi *et al*. in HEM material. This study shows that the cell efficiencies mainly depend on the quality of mc-Si wafer.

Cell 9: In 2004, O. Schultz (Schultz *et al.,* 2004a) reported an efficiency of 20·4%, which is the highest efficiency reported so far in mc-Si solar cells. Schultz used wet SiO_2 passivation instead of thermally grown SiO_2 because thermally grown oxide decreases the lifetime which further reduces the cell parameters (Macdonald and Cuevas , 2000; Schultz *et al.,* 2004b) The physical cause of thermal degradation is due to the dissociation of impurity precipitates which results in a greater concentration of interstitial impurities.

In this study, the authors have modeled the cell structures 1–9. Based on the understanding of processing steps used in the fabrication of the cells discussed earlier, they have modeled a cell structure so that high efficiency can be achieved in mc-Si solar cells. The aim is to move one step beyond what has been achieved so far in mc-Si solar cell technology so that the performance of mc-Si solar cells can approach that of solar cells made on single crystal silicon. The solar cell performance characteristics were modeled in PC1D (Clugston and Basore, 1996). PC1D is a software package that uses finite-element, drift-diffusion analysis to solve the fully coupled, two-carrier semiconductor transport equations in one dimension (Sana *et al.,* 1993).

2. Process steps: our modeled structure

The general fabrication technique for making solar cells from silicon material is well known. The particular processing steps which will be used in our modeled structure of a solar cell are as follows: (i) starting material: *p*-type silicon with resistivity 0·6 Ω-cm and thickness 150 μm, (ii) gettering process performed to remove both areal and in-depth non-uniformities, (iii) plasma texturing, (iv) P (phosphorous) diffusion (typically 900–950°C for 5–15 min), (v) junction isolation to remove *n* region from the wafer edges, (vi) hydrogenation for defect passivation, (vii) wet SiO_2 (Schultz *et al.,* 2004a) on front and back, (viii) AR coating of silicon nitride or TiO_2 to reduce reflection losses, (ix) photolithography on front side to make contact, (x) metallization on front side to make contact, (xi) photolithography on back side to make contact and (xii) firing to achieve proper back surface field (BSF).

In the modeled structure of mc-Si solar cell, the authors choose the above discussed processing steps. These are summarized in Figure 1.

Figure 2 shows the layout of the modeled structure. Selective metallization on the front and back help to improve passivation. The role of front and back surface passivation is important in the

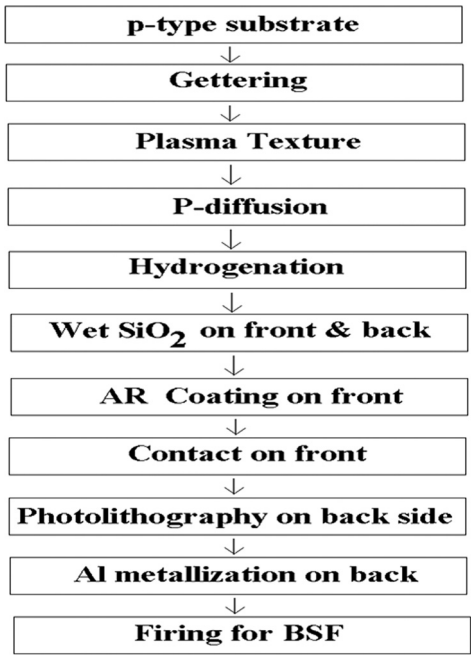

Figure 1. Processing steps in our structure.

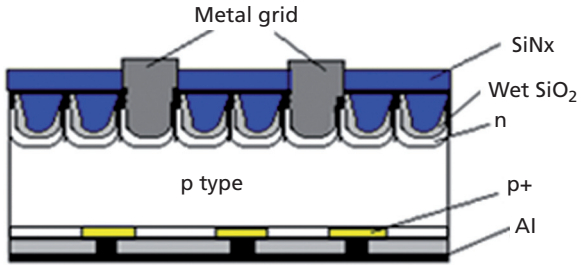

Figure 2. Final layout of our modeled structure.

present technology of mc-Si solar cells as the thickness of silicon wafer is reduced by the solar cell industry to reduce material costs. The effect of front and back surface recombination velocity on the performance on mc-Si solar cells has been discussed elsewhere (Budhraja *et al.,* 2011b).

3. Results: modeling

3.1 Details of modeling parameters used in our modeled structure

The modeling of structure as well as of the other cells was performed (i.e., cell 1–cell 9) using the PC1D modeling tool. The model parameters used for simulation of cell 1–9 was taken from the experimental data published by various groups. The details of parameters used for the modeling of the structure are given in this section. Since the solar cell industries have started to use thinner wafers to reduce cost, the thickness of *p*-type wafer was chosen to be 150 µm. The internal reflectance of the cell was taken to be 0·05.

Parameters for PCID

DEVICE
Device Area: 1 cm^2
Front surface Texture Angle: 54.74
Front surface barrer: 0.05 eV
Exterior Front reflectance: 0.05
Internal optical reflectance enabled
Front surface optically rough
Base contact: 1.5 X 10^{-3} ohm
Internal conductor: 3 X 10^{-5} S

REGION 1
Thickness : 150µm
Material used: Silicon
Carrier mobilities from internal model
Dielectric constant: 11.9
Bandgap: 1.1 eV
Intrinsic conc. at 300 K : 1X $10^{10}cm^{-3}$
Refractive index: Use standard file for silicon
Absorption coefficient: Use standard file for silicon
No free carrier absorption used
P-type background doping: 2.652 X $10^{16}cm^{-3}$
Front diffusion: N-type, $10^{19}cm^{-3}$
Rear diffusion: P-type, $10^{20}cm^{-3}$
Bulk recombination life time : 50 µs
Front surface recombination velocity: 1000 cm/s
Back surface recombination velocity: 1000 cm/s

EXCITATION
Excitation modified from one-sun.exc
Excitation mode: Transient, 16 timesteps
Temperature : 25^0C
Base circuit Sweep from -0.8 to 0.8 V
Constant intensity: 0.1 W cm^{-2}
Spectrum from am15g.spc

RESULTS
Short-circuit Ib : 39.39 amps
Max base power out : 2.194 watts
Open-circuit Vb: 0.6659 volts

Figure 3. Summary of parameters for PCID model.

For the bulk substrate, the standard properties of silicon were used. The standard data for the absorption coefficient and refractive index was used at 300K. The resistivity of the base substrate was taken to be 0·65 Ω cm with boron doping concentration of $2{\cdot}65 \times 10^{16}$ cm^{-3}. The bulk lifetime was taken to be 50 µs. In the world record cells, the research groups (Rohatgi *et al.,* 1996; Schultz *et al.,* 2004a; Zhao *et al.,* 1998) have used good quality bulk material made from several methods such as HEM, electromagnetic casting (EMC), direct solidification system (DSS) and so forth. The bulk lifetime in these materials is more than 100 µs but the authors choose the bulk lifetime to be 50 µs to show the modeling results for the worst case. Phosphorous diffusion was used on the front side to make an *n-p* junction. The peak doping concentration on the front side was taken to be 10^{19} cm^{-3}. The internal series resistance was chosen to be 1·5 mΩ on base contact. These values of resistances were taken from 16% efficiency mc-Si solar cells. The experimental data of these cells has been reported (Sopori, 2010). The front surface recombination velocity in *n*-region was varied from 10^3–10^6 cm/s. Similarly, the back surface recombination velocity in *p*-region was varied from 10^3–10^6 cm/s. The parameters used in PC1D are summarized in Figure 3.

3.2 Comparison of current density (*J*) – voltage (*V*) characteristics of our modeled structure with other world record cells

For the light *J-V* characteristics, the spectrum of air mass 1·5 (Website 1) was used in the PC1D modeling tool. This corresponds to a power density of 0·1 W/cm^2. The light *J-V* characteristic of our modeled structure (Figure 2) was compared with the light *J-V* characteristics of other cells discussed in section 1. This comparison is shown in Figure 4.

The values of cell parameters including short circuit current density (J_{sc}), open circuit voltage (V_{oc}), fill factor (FF) and efficiency for

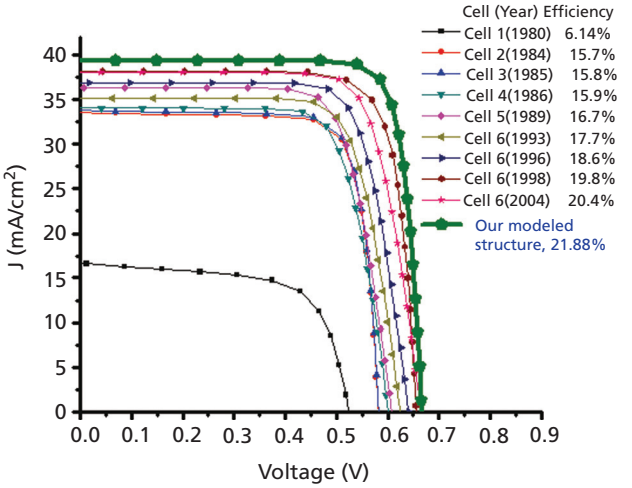

Figure 4. Simulated results of J-V characteristics of the modeled structure and other cells.

various cells and our modeled structure are shown in Table 1. Moreover, Table 1 summarizes the values of surface recombination velocity on the front surface (S_1) and on the back surface (S_2) used in the modeling. The values of cell thickness, resistivity, bulk lifetime, front doping concentration and sheet resistance for cells 1–9 were taken from the details of their references. There is negligible difference between the modeling results and experimental results of cell 1–9. The simulations based on PC1D are in excellent agreement with the experimental results. Based on these results, the modeling of our structure was done in PC1D.

3.2.1 Discussion on Table 1

There is increment in all cell parameters from cell 1 to cell 2. Insufficient passivation was used in cell 1. The high surface recombination limits high efficiency and other cell parameters in cell 1. The use of a low grade polycrystalline wafer was another reason for reduced performance in the fabrication of cell 1. There was a sudden jump in efficiency from cell 1 to cell 2. The pc-Si wafer with a grain size of 1–2 mm was used in the fabrication of cell 2 which increases the efficiency of cell 2. The effective diffusion length of the wafer used in the processing of cell 2 was more than the diffusion length of the wafer used in the processing of cell 1.

From cell 2 to cell 4, there is not too much change in cell parameters. The wafer quality and process steps used in the fabrication of cell 2, cell 3 and cell 4 were generally similar. The plasma treatments used in the fabrication of cell 3 helps to improve its efficiency from 15·7 to 15·8%. The plasma treatment step consists of plasma hydrogenation, plasma etching of cell emitter and plasma silicon nitride deposition which helps to increase cell performance parameters. The process steps in cells 3 and 4 were exactly the same except there is an additional step of phosphorous pretreatment in cell 4. Phosphorous pretreatment increases the effective diffusion length by the diffusion of phosphorous in the poor crystallographic regions of the wafer. Increase in diffusion length increases the efficiency by 0·1% in cell 4. There is not much difference in front and back surface recombination in cells 2, 3 and 4.

There was another increase in efficiency from cell 4 to 5. Laser texturing was used in the processing of cell 5 which increases

Cell no.	Year	J_{sc} (mA/cm²)	V_{oc} (V)	Fill factor	Efficiency (%)	S_1 (cm/s)	S_2 (cm/s)
1	1980	16·000	0·573	0·760	6·14	10^6	$1\cdot\times 10^6$
2	1984	33·675	0·609	0·779	15·70	10^4	$1\cdot\times 10^6$
3	1985	33·925	0·605	0·775	15·80	10^4	$1\cdot\times 10^5$
4	1986	34·032	0·605	0·781	15·90	10^4	$1\cdot\times 10^5$
5	1989	36·347	0·602	0·760	16·70	10^5	$1\cdot\times 10^4$
6	1993	35·170	0·623	0·794	17·70	10^4	$1\cdot\times 10^4$
7	1996	36·902	0·641	0·812	18·60	10^4	$2\cdot\times 10^3$
8	1998	38·178	0·656	0·802	19·80	10^3	$1\cdot\times 10^4$
9	2004	38·020	0·664	0·809	20·40	10^3	$1\cdot\times 10^3$
Our structure	2011	39·390	0·666	0·834	21·88	10^3	$1\cdot\times 10^3$

Table 1. Comparison of cell parameters of proposed structure with other cells.

optical absorption on the front surface. Instead of screen printing, patterning was used in cell 5 to make the front contact.

There is a 1% increment from cell 5 to 6. An emitter etch back technique was used to increase sheet resistance in the processing of cell 6. Moreover, the controlled back surface field helps to increase open circuit voltage in cell 6 resulting in significant improvement in V_{oc} and fill factor.

But for the bulk material, there were the same process steps used in the fabrication of cell 6 and cell 7. The bulk life time of the wafer used in cell 7 was larger than that of the wafer used in cell 6.

From cell 8 to 9, there was 1·2% increment in efficiency. Patterning was used on both the front and back surface in the processing of cell 9. The honeycomb texture used in the fabrication of cell 9 provides uniform texturing to increase multiple reflections on the front surface.

The processing of cell 9 provides good surface passivation on the front as well on the back surface. The wafer used in the fabrication of cell 9 was of better quality than that used for cell 8. The research group which processed cell 9 also attempted to fabricate a cell using the wafer (i.e., HEM; used in the fabrication of cell 8) and achieved efficiency of 18·2%. This indicates that the performance of the cell is mainly affected by the quality of the wafer.

There is very little change in efficiency and other performance parameters from cell 8 to 9. Instead of thermal oxidation, wet SiO_2 was used in the fabrication of cell 9. Thermal oxidation reduces the bulk lifetime which further affects the efficiency and other cell parameters.

In the proposed structure, the authors mainly focus on the importance of front and back surface recombination velocities. They have assumed the front and back surface recombination velocities to be 10^3 cm/s which are expected to be achieved experimentally. On the front, they selected uniform texture which helps to increase multiple reflections. Large grain size which reduces the grain boundary effects was selected (Ghitani and Martinuzzi, 1989; Halder and Williams, 1983). Features such as uniform texturing, high diffusion length, low lifetime, high sheet resistance, low surface recombination on front and back etc. were used in the modeling of the structure. The results of the modeled structure showed highest efficiency.

The dark current density (J) - voltage (V) curve fitting of the solar cells was performed using a two-diode model. The equation is as follows (Hussein *et al.,* 2001):

1. $$J = J_{01}\left\{\exp\left[\frac{q(V-R_sI)}{kT}\right]-1\right\}+J_{01}\left\{\exp\left[\frac{q(V-R_sI)}{2kT}\right]-1\right\}+\left(\frac{V-R_sI}{R_{sh}}\right)-J_L,$$

Solar cell	R_s (Ω.cm²)	R_{sh} (kΩ)	J_{01} (mA/cm²)	J_{02} (mA/cm²)
Cell 1	2·87	0·30	$2{\cdot}68 \times e^{-09}$	$2{\cdot}03 \times e^{-07}$
Cell 2	2·15	3·01	$5{\cdot}96 \times e^{-09}$	$3{\cdot}40 \times e^{-07}$
Cell 3	2·13	3·04	$5{\cdot}71 \times e^{-09}$	$3{\cdot}43 \times e^{-07}$
Cell 4	2·12	3·84	$1{\cdot}73 \times e^{-09}$	$4{\cdot}60 \times e^{-07}$
Cell 5	1·51	25·40	$1{\cdot}64 \times e^{-09}$	$3{\cdot}48 \times e^{-07}$
Cell 6	1·52	34·53	$7{\cdot}69 \times e^{-09}$	$2{\cdot}45 \times e^{-07}$
Cell 7	1·52	54·56	$8{\cdot}83 \times e^{-09}$	$5{\cdot}85 \times e^{-07}$
Cell 8	1·51	54·78	$4{\cdot}44 \times e^{-09}$	$4{\cdot}10 \times e^{-06}$
Cell 9	1·48	55·95	$2{\cdot}01 \times e^{-09}$	$1{\cdot}26 \times e^{-06}$
Our structure	1·37	60·00	$1{\cdot}89 \times e^{-09}$	$1{\cdot}20 \times e^{-06}$

Table 2. Parameters obtained from dark *J-V* characteristics.

where, J_{01} and J_{02} are the saturation current densities, k is Boltzman's constant, T is the temperature, q is the electronic charge, R_s is the series resistance, R_{sh} is the shunt resistance and J_L is the light induced current density and it equals to zero in dark conditions.

Solar cell performance parameters such as J_{01}, J_{02}, R_s, R_{sh} were calculated from the dark I–V curves and are shown in Table 2. The first term in Equation 1 is due to the recombination current in the quasi neutral region (from first diode) and the second term is due to the recombination current in the depletion region (from the second diode). The value of series resistance (R_s) decreases and shunt resistance (R_{sh}) increases from top to bottom in Table 2. This is in agreement with the explanation that high value of series resistance and low value of shunt resistance corresponds to the low performance of the cell.

3.3 Effect of front surface passivation in our modeled structure

The possible processing techniques for front surface passivation that have been followed by various research groups are thermal oxidation, selective metallization, SiN_x:H passivation, etc. Front surface recombination velocity (S_1) is an important parameter to measure the passivation at the front surface. Figure 5(a) shows the variation in *J-V* characteristics with respect to S_1. For most semiconductors, the surface recombination velocity is of the order of 10^7 cm/s (Website 2) but, experimentally, it has become possible to reduce the value of S_1 to 10^3 cm/s (Rohatgi *et al.,* 1996; Sana *et al.,* 1993; Schultz *et al.,* 2004a). As the front surface recombination velocity increases, the value of cell performance parameters such

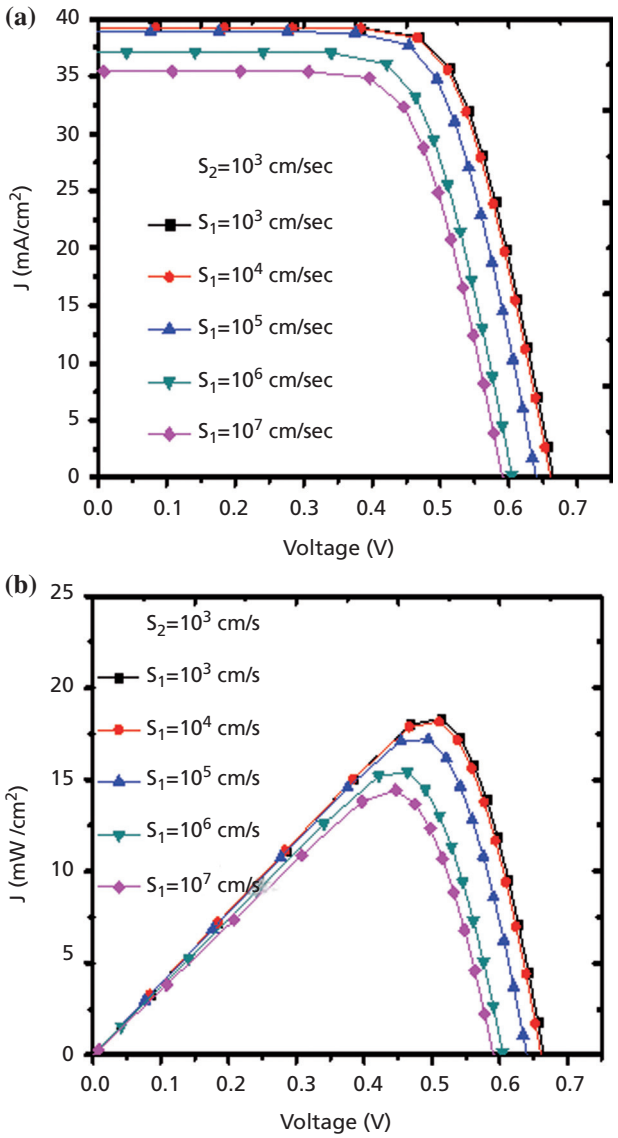

Figure 5. (a) Simulated *J-V* characteristics and (b) Power density against voltage for various values of S1.

Back surface recombination velocity (cm/s)	J_{sc} (mA/cm²)	V_{oc} (V)	Fill Factor	Efficiency (%)
$S_2 = 10^3$	39·39	0·666	0·834	21·88
$S_2 = 10^4$	39·35	0·665	0·833	21·83
$S_2 = 10^5$	39·2	0·662	0·833	21·62
$S_2 = 10^6$	39·1	0·659	0·831	21·47

Table 3. The values of cell parameters in the modeled structure for different values of S_1; S_2 = 10³ cm/s in all cases.

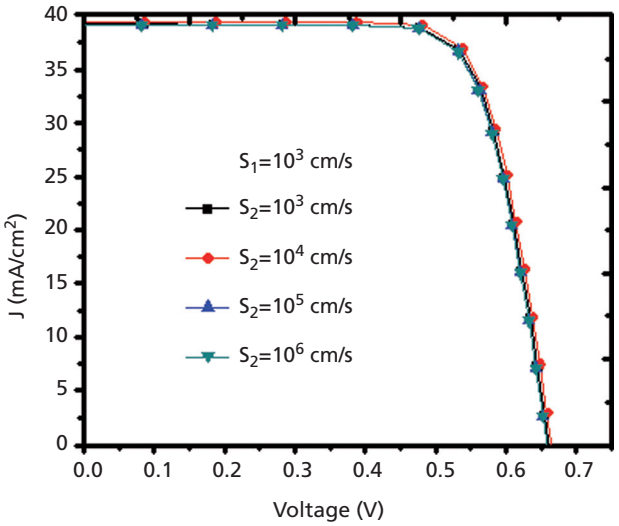

Figure 6. J-V characteristics for various values of S2.

as J_{sc}, V_{oc}, fill factor and efficiency decreases. Table 3 shows the calculated values of the cell parameters.

The power density also reduces as S_1 increases (as shown in Figure 5(b)). The maximum power density is shifted towards higher voltages. At lower values of front surface recombination velocity, the value of power density is higher at all voltages. This is because, as S_1 increases, the carriers start recombining at the front surface which reduces the current and other associated cell parameters. In this structure, the authors select oxidation and metallization followed by photolithography on the front surface. The metal contact helps to collect carriers and SiO_2 reduces the recombination on the front surface. SiN_x, along with SiO_2, helps in passivation as well as providing a suitable AR coating to increase absorption.

3.4 Effect of back surface passivation in the modeled structure

The passivation techniques used on the back surface are back surface field, oxidation, etc. In this structure, the authors select wet oxidation followed by photolithography. Photolithography is used for selective opening so that the metallization can be performed to obtain a suitable back surface field. The parameter which measures the back surface passivation is the back surface recombination velocity (S_2). Figure 6 shows the variation in *J-V* characteristics with respect to S_2. The variation in current density is very small with respect to S_2. The variation in spectral response with respect to S_2 has been shown elsewhere (Budhraja *et al.,* 2011b). This also confirms that the difference in cell parameters with respect to S_2 is

Front surface recombination velocity (cm/s)	J_{sc} (mA/cm²)	V_{oc} (V)	Fill factor	Efficiency (%)
S1 = 103	39·39	0·666	0·834	21·88
S1 = 104	39·35	0·662	0·833	21·71
S1 = 105	38·18	0·640	0·824	20·07
S1 = 106	37·22	0·605	0·822	18·53
S1 = 107	35·56	0·591	0·819	17·22

Table 4. The values of cell parameters in the proposed structure for various values of S_2, S_1 = 103 cm/s in all cases.

very small. However, its significance at the front surface determines the large variation in current density with respect to front surface recombination velocity.

As the back surface recombination velocity increases, the value of cell performance parameters decreases but the difference in magnitude is very small in comparison to those that correspond to the front surface recombination velocity. The values of the cell parameters for various values of S_2 are summarized in Table 4. There is a small change in efficiency from 21·88 to 21·47% as S_2 changes from 10^3 to 10^6 cm/s. Similarly, there is a small change in other cell parameters with respect to the change in S_2. The effect of S_2 in thick solar cells is very small because the generation rate becomes very small at the back surface. The minority carriers which are generated close to the back surface are not able to reach the junction if the wafer is thick enough. The role of back surface passivation will be more significant when the solar cell industries start to utilize thin wafers to reduce cost (Ravi, 2011) because, in thin wafers, the diffusion length of carriers is enough to reach the junction. The carriers will recombine at the back surface instead of reaching the junction if the back surface recombination velocity is high. The open-circuit voltage will also increase in thin wafers if the proper back surface field is available on the back surface. The back surface field has a net effect of passivating the back surface, especially when the wafer is thin.

4. Conclusions

J-V characteristics of various mc-Si solar cells were modeled and compared in PC1D software. It was confirmed that PC1D was able to simulate the experimental results for various mc-Si solar cells that have been reported by a number of research groups. The modeling of the proposed structure of the mc-Si solar cell was performed in PC1D. Based on the understanding and the literature survey, the authors chose processing steps which are able to yield high efficiency in mc-Si solar cells.

The modeling of the proposed structure of mc-Si solar cell gives J_{sc} = 39·39 mA/cm², V_{oc} = 0·666 V, fill factor = 0·834 and efficiency = 21·88%. Other parameters such as series resistance, shunt resistance, saturation current densities, etc. were also calculated from the dark *J-V* characteristics for various cells from the two-diode model.

It is important to have the proper front and back surface passivation, especially when the solar cell industries are moving towards the use of thinner wafers to reduce cost. Parameters such as front and back surface recombination velocities were used to quantify the front and back surface passivation respectively. In mc-Si solar cells, the front and back surface recombination velocities are very high, i.e. ≥ 10^6 cm/s, but it can be reduced to ≤ 10^3 cm/s by using passivation techniques such as SiN_x:H deposition, oxidation and back surface field. There was more effect of front surface recombination velocity on the performance of solar cells than back surface recombination velocity. The role of back surface recombination velocity will be significant if the wafer gets thinner. The change in spectral response with respect to S_2 will be more pronounced (Budhraja *et al.,* 2011c) when the thickness of the cell is further reduced by the solar cell industry. This is because of the fact that, in thinner wafers, the generation rate will be significant at the back surface and can no longer be neglected.

The modeling results of the proposed structure of the mc-Si solar cell are encouraging and should lead to improvement in design, fabrication, performance characteristics and efficiencies of mc-Si cells.

Acknowledgements

The authors thank Dr. Ana Kanevce and Dr. Bhushan Sopori of National Renewable Energy Laboratory for their valuable input. The authors would also like to gratefully acknowledge the financial support rendered by the US Department of Energy for this contribution.

REFERENCES

Basore P (1994) Defining terms for crystalline silicon solar cells, progress in photovoltaics: research and applications **2**: 177–179.

Budhraja V, Misra D and Ravindra NM (2011a) Advancements in PV multicrystalline silicon solar cells from 1980 to 2010 — An overview. 37th IEEE PVSC, Seattle, Washington, pp. 19–24.

Budhraja V, Sopori B, Ravindra NM and Misra D (2011b) An improved model of dislocations in a silicon solar cell. 21st Workshop on crystalline silicon solar cells & modules: Materials and processes, Breckenridge, Colorado, pp.158-159.

Budhraja V, Sopori B, Ravindra NM and Misra D (2011c) Improved dislocation model of silicon solar cells with the effect of front and back surface recombination velocity. (in press).

Clugston D and Basore P (1996) PC1D Version 5: 32-bit solar cell modeling on personal computers. 26th IEEE Photovoltaic Specialists Conference Anaheim CA, pp. 207–210.

Ghitani HEl and Martinuzzi S (1989) Influence of dislocations on large grained polycrystalline silicon cells. I.Model. *Journal of Applied Physics* **66**: 1717–1722.

Green MA, Blakers AW, Jiqun S, Keller EM and Wenham SR (1984) 19.1% efficient silicon solar cell. *Applied Physics Letters* **44**: 1163–1164.

Halder NC and Williams TR (1983) Grain boundary effects in polycrystalline silicon solar cells I: Solution of the three dimensional diffusion equation by the green's function method. *Solar Cells* **8**: 201–223.

Hussein R, Borchert D, Grabosch G and Fahrner WR (2001) Dark I-V-T measurements and characteristics of (n) a-Si/(p) c-Si heterojunction solar cells. *Solar Energy Materials and Solar Cells* **69**: 123–129.

Johnson SM and Winter C (1984) High efficiency large area polysilicon solar cells. IEEE 17th PVSC 1121–1126.

Macdonald D and Cuevas A (2000) The trade-off between phosphorous gettering and thermal degradation in multicrystalline silicon. 16th European Photovoltaic Solar Energy Conference. pp. 1707–1710.

Magazine Article (2011) "C-Si Putting Pressure On Thin Films", January. *Solar Industry*: 4.

Narayanan S, Wenham SR and Green MA (1986) High efficiency polycrystalline silicon solar cells using phosphorous pretreatment. *Applied Physics Letters* **48**: 873–875.

Ravi KV (2011) Poly-less, ingot-less, kerfless production of very thin (<50 microns) single crystal single wafers, solar cells and modules. 21st Workshop on crystalline silicon solar cells & modules: materials and processes, Breckenridge, Colorado, July 31–August 3.

Rohatgi A, Narasimha S , Kamra S *et al*. (1996) Record high 18.6% efficiency solar cell on HEM multicrystalline material. 25th IEEE PVSC 741–744.

Saitoh T, Warabisako T, Kuroda E *et al*. (1980) Impurity gettering of polycrystalline solar cells fabricated from refined metallurgical-grade silicon. *IEEE Transaction on Electron Devices* **27**: 671–677.

Sana P, Salami J and Rohatgi A (1993) Fabrication and analysis of high-efficiency polycrystalline silicon solar cells. *IEEE Transaction on Electron Devices* **40**: 1461–1468.

Schultz O, Gluntz SW and Willeke GP (2004a) Multicrystalline silicon solar cells exceeding 20% efficiency. *Progress in Photovoltaics Research and Applications* **12**: 553–558.

Schultz O, Riepe S and Glunz SW (2004b) Influence of high temperature processes on multicrystalline silicon. *Solid State Phenomena* **95/96**: 235–240.

Sopori B, Rupnowski P, Shet S *et al.* (2010) Influence of defects and defect distributions in multicrystalline silicon on solar cell performance. 35th IEEE PVSC, Honolulu, Hawai, June 20–25, pp. 2233–2237.

Tobias I,Canizo CD and Alonso J (2004) *Handbook of Photovoltaic Science and Engineering,* Chapter 7**,** pp. 254–307. Website 1: http://rredc.nrel.gov/solar/spectra/am1.5/; Website 2: http://pveducation.org/pvcdrom/pn-junction/surface-recombination.

Wenham SR, Willison MR, Narayanan S and Green MA (1985) Efficiency improvement in screen printed polycrystalline silicon solar cells by plasma treatment. 18th IEEE PVSC 1008–1013.

Wu B, Stoddard N, Ma R and Clark R. Bulk multicrystalline silicon growth for photovoltaic (PV) application. *Journal of Crystal Growth* **310**: 2178–2184.

Zhao J, Wang A, Green MA and Ferrazza F (1998) 19.8% efficient honeycomb textured multicrystalline and 24.4% monocrystalline silicon solar cells. *Applied Physics Letters* **73**: 1991–1993.

Zolper JC, Narayanan S, Wenham SR and Green MA (1989) 16.7% efficient, laser textured, buried contact polycrystalline silicon solar cell. *Applied Physics Letters* **55**: 2363–2365.

WHAT DO YOU THINK?

To discuss this paper, please email up to 500 words to the managing editor at emr@icepublishing.com

Your contribution will be forwarded to the author(s) for a reply and, if considered appropriate by the editor-in-chief, will be published as a discussion in a future issue of the journal.

ICE Science journals rely entirely on contributions sent in by professionals, academics and students coming from the field of materials science and engineering. Articles should be within 5000-7000 words long (short communications and opinion articles should be within 2000 words long), with adequate illustrations and references. To access our author guidelines and how to submit your paper, please refer to the journal website at www.icevirtuallibrary.com/emr